Stochastic Threshold for Ion Heating with Beating Electrostatic Waves

B. Jorns and E. Y. Choueiri

Electric Propulsion and Plasma Dynamics Laboratory (EPPDyL), Princeton University, Princeton, New Jersey 08544, USA

(Received 10 January 2013; published 14 June 2013)

The stochastic threshold for the heating of ions in a magnetized plasma with two electrostatic waves is experimentally characterized. Two obliquely propagating electrostatic modes are launched in a magnetized plasma with frequencies that differ by the ion cyclotron frequency. The values of the wave amplitudes where a rapid increase in the local ion temperature occurs is then parametrically investigated. It is found that the two threshold wave amplitudes are linearly related and that this dependence translates to a lower required energy density for the onset of heating when compared to the case of a single electrostatic wave. Agreement also is demonstrated between the experimentally observed threshold for stochastic heating and an analytical prediction [B. Jorns and E. Y. Choueiri, Phys. Rev. E **87**, 013107 (2013)] for this threshold.

DOI: 10.1103/PhysRevLett.110.245002 PACS numbers: 52.35.Fp, 52.35.Mw, 52.50.Qt

The onset of irreversible ion heating by electrostatic waves in a magnetized plasma depends on the existence of a mechanism to effectively randomize particle orbits. For monochromatic waves with sufficiently large wave amplitudes, one such mechanism for achieving this end is the onset of stochasticity in orbits [1–4] where the subsequent diffusion in velocity and thermalization of the population produces a marked increase in ion temperature [5,6]. For both oblique and perpendicular single electrostatic waves (SEW), this stochastic heating only occurs when the wave amplitude exceeds a minimum value [2,4]. This threshold corresponds to the limit where the acceleration from the wave is sufficient to decorrelate the phase between the wave and ion's cyclotron orbit. A similar decorrelating effect can be achieved by introducing a second wave to the system [7,8]. The additional perturbations to the particle orbit produced by the interaction of the two waves lead to stochastic effects even when the amplitudes of the individual waves are lower than the SEW threshold value. This is an important characteristic that recommends a two-wave heating process over SEW when the perturbation strength of individual modes is limited by saturation effects in the plasma. Moreover, when the two waves are properly conditioned [8], this lower amplitude requirement can translate directly to stochastic onset for a lower total wave energy density. Since the onset of heating is correlated with stochasticity, this attribute suggests the two-wave process may be more efficient for heating.

One two-wave interaction that has been identified to confer both the advantage of lower individual wave amplitudes and a lower total energy density for stochastic onset is ion heating by beating electrostatic waves (BEW) [8]. This low-threshold process has applications ranging from space plasmas where it may serve as a driver for anomalous ion transport in the Earth's ionosphere [9] to applications in the laboratory where its potential for efficient ion heating is well suited for both low-temperature plasma processing and electric propulsion. The BEW process is characterized by two modes that satisfy the so-called beating criterion, $f_2 - f_1 = nf_{ci}$, where f_1, f_2 denote the wave frequencies, f_{ci} is the ion cyclotron frequency, and n is an integer [10–14]. At sufficiently large wave amplitudes, the natural resonance between the beat frequency of the two waves and the ion cyclotron frequency is predicted to lead to a linear dependence in wave amplitude for the onset of stochasticity. This linearity in turn corresponds to a lower required energy density for stochastic onset than in the SEW case [8]. Assuming this stochasticity results in enhanced ion heating, we therefore anticipate that the start of ion heating—noted by a jump in ion temperature above background—will also be linear in wave amplitude and occur at lower energy densities than heating with the SEW process. In this Letter, we experimentally examine these conclusions by exploring the amplitude and energy density dependence of where the threshold in heating occurs for the BEW process and comparing it with the analytically predicted results derived in Ref. [8].

The trials we report here were performed on the Beating Waves Experiment II (BWX II) [15], an axially symmetric, uniformly magnetized argon plasma sustained by an inductive, radio frequency discharge. In BWX II, the plasma is contained by a Pyrex cylinder 132 cm in length with a 16.5 cm inner diameter placed concentrically in a 122 cm long, 10 ring solenoid. This configuration provides a uniform magnetic field of 525 G with corresponding cyclotron frequency $f_{ci} = 20$ kHz. The experiments were performed at a background pressure of 0.1 mTorr and a rf power of 275 W that provided an approximately uniform plasma density $n_i \approx 10^{11}$ cm^{-3} out to 3 cm from the plasma center. All measurements were made at this radius. The background temperatures of each species in the plasma were observed to be $T_{e0} \approx 3.5$ eV and $T_{i0} \approx 0.25$ eV.

Two electrostatic modes were launched inductively from outside the plasma by a single strap antenna, 5.5 cm wide and 25 cm in length with the longer axis oriented parallel to the magnetic field. Maximal power was coupled into each excited mode by means of the variable dual-frequency matching network described in Ref. [16]. In order to determine the properties of the propagating waves, we measured the dielectric response of the ion population by means of a laser induced fluorescence system tuned to the Ar II ion transition at 668.614 nm [17]. Fitting a theoretical model to this measured response yielded a local estimate for the wave vectors of the propagating modes [18,19]. We similarly estimated the potential amplitudes of the waves by calculating the magnitude of the density perturbation from the dielectric response [19].

We show in Fig. 1 the measured values of the perpendicular $k_\perp$ and parallel k_z wave vectors of the launched modes in the BWX II plasma as functions of the normalized angular frequency ω/Ω_i, where $\Omega_i = 2\pi f_{\mathrm{ci}}$. The near acoustic relationship in this figure with a cutoff at the cyclotron frequency suggests that the excited mode is the electrostatic ion cyclotron wave [20], a low-frequency wave that has been observed in comparable experimental configurations [19]. Similarly, the parity between the perpendicular wavelengths and the plasma radius indicates that the propagating waves are bounded eigenmodes. In order to facilitate a comparison between the stochastic onset created by these bounded modes and the theoretical threshold from Ref. [8] that assumes the BEW are locally planar, we constrained our experimental measurements to $r < 3$ cm. This is the region of uniform plasma parameters where we have concluded through a combination of antenna-coupling simulations and a second set of wave measurements at $r = 0$ that the waves can be approximated as locally planar. In this region, we also have found that for $\omega \geq 2\Omega_i$, the perpendicular components of the propagating modes are collinear and normal to the antenna.

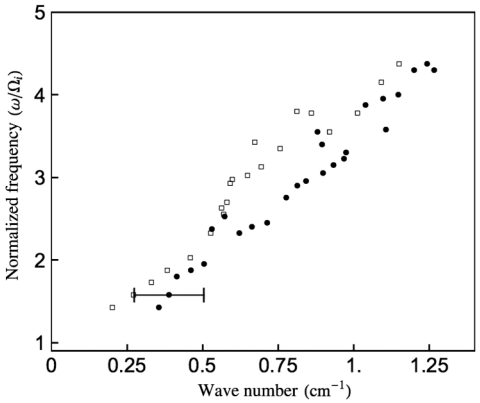

FIG. 1. Experimentally determined dispersion relation for the perpendicular (closed circle) and parallel (open square) components of the wave vector. A representative error bar is also shown.

As for wave accessibility, we note that while the ion-momentum collision frequency ν_i is sufficiently large in the BWX II plasma ($\nu_i/\Omega_i \approx 0.1$) to lead to light spatial damping of the propagating modes, we found that the wave potential amplitudes remained sufficiently large in the experimentally observed region to permit an investigation of the theoretically predicted stochastic threshold. Similarly, given the large disparity between electron thermal velocity and the wave phase velocity, we neglected collisionless electron heating as a source for ion heating. We also ruled out stochastic heating from electrons since the inverse dependence on species mass of the threshold for stochastic onset [8] suggests that the wave amplitudes we investigated for the onset of stochastic ion heating were well below the threshold for electrons. The negligible role of electron heating was supported by our observation that the electron temperature remained constant at all threshold ion-heating conditions.

We measured ion temperature in this experiment by examining the Doppler broadening of the transition line with the aforementioned laser induced fluorescence system. With this method, a scan of SEW heating from $\omega_1 = \Omega_i - 5\Omega_i$ for equal power input to the strap antenna revealed maximal heating at $\omega = 2\Omega_i$. We therefore chose the frequency combination $\omega_1 = 2\Omega_i$, $\omega_2 = 3\Omega_i$ with associated wave numbers $k_{1\perp} = 60$ m^{-1}, $k_{1z} = 43$ m^{-1} and $k_{2\perp} = 85$ m^{-1}, $k_{2z} = 56$ m^{-1} for our BEW investigation. With this frequency set, we proceeded to estimate the threshold for the onset of heating by incrementally increasing the current to the antenna at each BEW frequency, I_1, I_2, and measuring the equilibrated temperature. Three representative data sets are shown in Fig. 2 where each trend corresponds to a different fixed value of I_2. It is evident from these plots, similar to those reported in

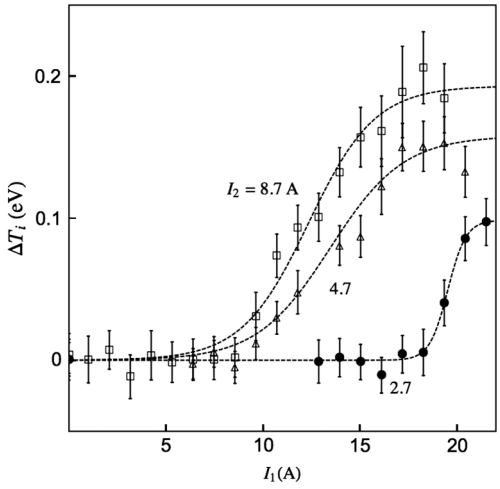

FIG. 2. Change in ion temperature as a function of input current I_1 to the lower frequency mode. Each data set corresponds to a fixed level of current in the second mode I_2. The dotted lines are best fits from Eq. (1), a phenomenological model for the heating.

Refs. [5,6], that there is a threshold value where a jump in temperature above background occurs. This is followed by a rapid increase with antenna current that ultimately gives way to saturation for sufficiently large values—a result that likely stems from either enhanced loss processes or self-consistent effects in the plasma that prevent further energy exchange of the mode with the ions. As is intuitively expected, we can see from Fig. 2 that the threshold value I_1 decreases with larger values of I_2.

In order to quantify the value where the onset of heating occurs, we numerically applied the following phenomenological trend to the increase in temperature over background:

$$\Delta T_i = T_i - T_{i0} = \Delta T_s(\tanh[AI_1 + I_0] + 1), \quad (1)$$

where ΔT_s, A, and I_0 are free parameters. We subsequently identified the threshold for heating as the current value where according to Eq. (1) the temperature is 10% of the saturated value, i.e., where $(T_i - T_{i0})/\Delta T_s = 0.1$. This is an appropriate metric as it controls for the fact that the magnitude of temperature increase—once heating has onset—is also heavily dependent on the antenna current. We employed a previously generated calibration curve in order to relate the measured currents I_1, I_2 to the wave potential amplitudes, Φ_1, Φ_2.

Using the 10% metric as the criterion for heating onset, we show in Fig. 3 the threshold values of the potential amplitudes Φ_1, Φ_2 where the error in these plots reflects the uncertainty in relating the current to the measured wave amplitudes. As we have assumed that the threshold for heating is correlated with the appearance of stochasticity in ion orbits, these data confirm the two analytically predicted characteristics for the onset of BEW heating that we cited from Ref. [8]. First, the requisite amplitudes for producing stochasticity with BEW are lower for the individual waves when compared to SEW heating, i.e., where $\Phi_1 \to 0$ or $\Phi_2 \to 0$. Second, the relationship between threshold amplitudes is linear, which suggests that the onset of heating can be achieved for a lower total energy density than in the SEW case. We can confirm this second observation explicitly by estimating the total energy density in the system and comparing it to the onset condition for the SEW condition. To this end, we use the formula for the energy density for the acousticlike mode observed in BWX II [21]

$$W_j = \epsilon_0 \frac{\omega_j}{4} \Phi_j^2 \frac{\partial}{\partial \omega_j} D(\omega_j, \mathbf{k}_j), \quad (2)$$

where $D(\omega, \mathbf{k})$ stems from the electrostatic dispersion relation and is given by [21]

$$D(\omega, \mathbf{k}) = k_z^2 + k_\perp^2 + \sum_{s=e,i} k_{ds}^2 \Big[1 + \sum_n e^{-a_s} I_n(a_s) Z(\zeta_n) \times \Big(\zeta_n + \frac{n\Omega_s}{\sqrt{2} k_z v_{t(s)}} \Big) \Big]. \quad (3)$$

Here I_n is the modified Bessel function of the first kind; $k_{ds}^2 = n_s q^2/\epsilon_0 T_s$; $\zeta_n = (\omega - n_s\Omega_s - k_z v_{d(s)})/\sqrt{2} k_z v_{t(s)}$; $a_s = (k_\perp \rho_s)^2$; $\rho_s = v_{t(s)}/\Omega_s$; and $Z(\zeta_n) = 1/\sqrt{\pi} \int_{-\infty}^{\infty} [e^{-s^2}/(s - \zeta_n)] ds$, the plasma dispersion function. In these expressions, $v_{t(s)}^2 = T_s/m_s$ is the thermal velocity; m_s is the species mass; $v_{d(s)}$ is the drift velocity; n_s is the plasma density; q is the species charge; and ϵ_0 is the permittivity of free space.

By employing the dispersion relation for the electrostatic modes given by Eq. (3) and our observed amplitudes in Fig. 3, we use Eq. (2) to show in Fig. 4 the total energy density required for heating onset in the BEW case, $W_1 + W_2 = W_{\mathrm{BEW}}$, where the error bars stem from uncertainty

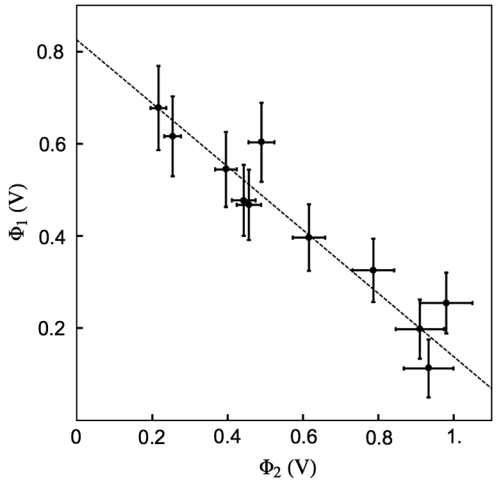

FIG. 3. Potential amplitudes of the two waves where the threshold for ion heating is observed to occur. The dotted line is a best-fit trend.

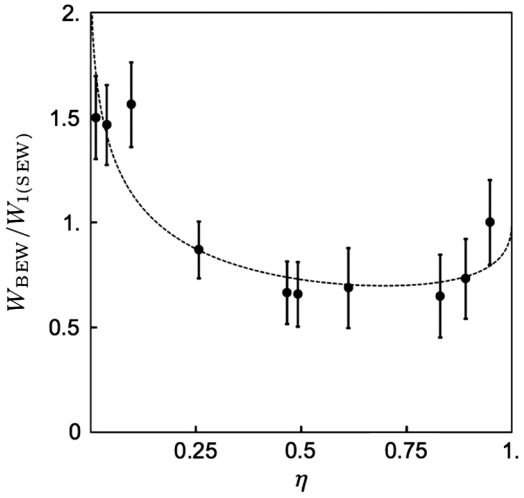

FIG. 4. Normalized total energy density where the threshold for ion heating is observed to occur as a function of the fraction of energy density in the first mode $\eta = W_1/W_{\mathrm{BEW}}$. The dotted line represents a best fit according to model Eq. (8).

both in the wave amplitudes and wave vectors. In this plot, the energy densities have been normalized by the required energy density $W_{1(\mathrm{SEW})}$ for onset with a SEW at ω_1, and the independent variable is $\eta = W_1/W_{\mathrm{BEW}}$, the fraction of the total BEW power in the first mode. It is evident from this figure that there exists a range $\eta \in (0.25, 1)$ where the threshold for the onset of heating is lower than that exhibited by either SEW case ($\eta = 0, 1$). This confirms that heating onset occurs for a lower total energy density with BEW than with a SEW.

With the observation of the BEW trends that were predicted in Ref. [8]—the linear relationship between the threshold amplitudes and the lower requisite energy density for onset—we are now in a position to explicitly compare the results from Figs. 3 and 4 with the analytical predictions from this previous work. From Eq. (32) in Ref. [8], we have the threshold for BEW stochastic acceleration for an ion with initial velocity $v_\perp$, v_z is given in physical coordinates by

$$\alpha = \frac{\omega_1 - k_z v_z}{\Omega_i B_0 v_\perp} k_{1\perp} (\Phi_1 |H^{(1)'}_{\mu_1}(z_1)| + \Phi_2 |H^{(1)'}_{\mu_2}(z_2)|), \tag{4}$$

where $H^{(1)}_{\mu_j}$ is the Hankel function of the first kind, B_0 denotes the background magnetic field magnitude, $\mu_j = (\omega_j - k_z v_z)/\Omega_i$, $z_j = k_{j\perp} v_\perp/\Omega_i$, and $\alpha = 0.17 \pm 0.1$ is a constant. This relationship was shown to be valid under the assumption that the perpendicular components of the two modes $k_{1\perp}$, $k_{2\perp}$ are collinear and that the parallel components satisfy $k_{1z} \approx k_{2z}$. Both of these assumptions are approximately valid for the two modes at $\omega_1 = 2\Omega_i$ and $\omega_2 = 3\Omega_i$. Similarly, since $\omega_1/k_{1z}/\bar{v}_z > 4$ where $\bar{v}_z = (2T_i/m_i)^{1/2}$ for our experimental configuration, we further make the simplifying assumption $\mu_j \approx \omega_j/\Omega_i$. Coupled with the fact that $\omega_1/k_{1\perp} \approx \omega_2/k_{2\perp}$ for our two modes, this approximation allows us to use the reduced form of Eq. (4) [Eq. (22) in Ref. [8]] in estimating the onset of stochasticity:

$$\alpha = \frac{k_{1\perp}^2}{\omega_1 B_0} \left[\Phi_1 \left(\frac{\omega_1}{\Omega_i}\right)^{1/3} + \Phi_2 \left(\frac{\omega_2}{\Omega_i}\right)^{1/3} \right]. \tag{5}$$

We then can relate the threshold values of the wave potential amplitudes by solving for Φ_1 as a function of Φ_2:

$$\Phi_1 = -a\Phi_2 + b, \tag{6}$$

where we have defined

$$a = \left[\frac{\omega_2}{\omega_1}\right]^{1/3}, \qquad b = \frac{\alpha B_0 \omega_1}{k_{1\perp}^2} \left(\frac{\Omega_i}{\omega_1}\right)^{1/3}. \tag{7}$$

As evidenced by Eq. (6), we now can see explicitly how the linear relationship between potential amplitudes in Fig. 3 follows the analytical prediction. Allowing a and b to be free parameters in a best fit to the data yields values for the coefficients $a = 0.7$ and $b = 0.8$. By comparison, we can calculate the analytically predicted values for a and b by substituting the wave parameters employed in our study, ω_1, ω_2 and $k_{1\perp}$, $k_{2\perp}$ into Eq. (7). This yields $a = 1.1$ and $b = 1 \pm 0.4$, where the uncertainty stems from errors in the wave number measurements as well as the spread in the theoretically derived value of α. We thus see that in spite of the assumptions we have made to place Eq. (6) in its simplified form, the observed linear relationship between the threshold wave amplitudes, as represented by the coefficients of the dotted line in Fig. 3, corresponds closely to the analytically derived forms of a and b. This relative agreement lends experimental weight to the theoretical analysis from Ref. [8].

The experimental agreement theory extends to our energy density analysis as well. From Eq. (26) in Ref. [8], we see the predicted normalized threshold in energy density is given by

$$\frac{W_{\mathrm{BEW}}}{W_{1(\mathrm{SEW})}} = [\sqrt{\eta} + \gamma\sqrt{1-\eta}]^{-2}, \tag{8}$$

where under the same assumptions we employed to derive Eq. (6), we have $\gamma = (\omega_2/\omega_1)^{1/3}(\beta_1/\beta_2)^{1/2}$ with $\beta_j = W_j/\Phi_j^2$. We calculate β_j from Eqs. (2) and (3) by letting $\Phi_j \to 1$ and employing our experimentally observed values for $\mathbf{k}_j$. These coefficients in turn correspond to the predicted value $\gamma = 0.91 \pm 0.3$ where the error stems from uncertainty in the detected wave number. For comparison, we fit Eq. (8) to the data in Fig. 4 to yield the dotted line shown, which has the best-fit parameter $\gamma = 0.64$. Once again, we find the model and experimental data agree to within error.

In sum, we have identified experimentally two trends for the BEW process: the onset of stochasticity is linear with respect to the perturbation amplitudes and the combination of BEW has a lower requisite total energy density to produce stochasticity than a SEW. Furthermore, we have found that the linear relationship between potential amplitudes as well as the dependence of the stochastic threshold on the BEW energy density correspond to within an order of magnitude to the analytical predictions in Ref. [8]. Thus, while our observed trends confirm experimentally that the onset of stochastic heating can be achieved more easily with BEW than with SEW, the quantitative agreement of the observed trends with analytical predictions lends support to the conclusions of our work in Ref. [8] about the driving mechanisms of the BEW process.

[1] C. Karney and A. Bers, Phys. Rev. Lett. **39**, 550 (1977).
[2] C. Karney, Phys. Fluids **21**, 1584 (1978).
[3] A. Fukuyama, H. Momota, R. Itatani, and T. Takizuka, Phys. Rev. Lett. **38**, 701 (1977).
[4] G. R. Smith and A. N. Kaufman, Phys. Rev. Lett. **34**, 1613 (1975).

[5] F. Skiff, F. Anderegg, and M. Q. Tran, Phys. Rev. Lett. **58**, 1430 (1987).
[6] A. Fasoli, F. Skiff, R. Kleiber, M. Q. Tran, and P. J. Paris, Phys. Rev. Lett. **70**, 303 (1993).
[7] Z. Sheng, L. Yu, G. Hao, and R. White, Phys. Plasmas **16**, 072106 (2009).
[8] B. Jorns and E. Y. Choueiri, Phys. Rev. E **87**, 013107 (2013).
[9] A. Ram, A. Bers, and D. Benisti, J. Geophys. Res. **103**, 9431 (1998).
[10] D. Benisti, A. K. Ram, and A. Bers, Phys. Plasmas **5**, 3224 (1998).
[11] D. Benisti, A. K. Ram, and A. Bers, Phys. Plasmas **5**, 3233 (1998).
[12] P. Chia, L. Schmitz, and R. Conn, Phys. Plasmas **3**, 1545 (1996).
[13] D. J. Strozzi, A. K. Ram, and A. Bers, Phys. Plasmas **10**, 2722 (2003).
[14] R. Spektor and E. Y. Choueiri, Phys. Rev. E **69**, 046402 (2004).
[15] B. Jorns and E. Choueiri, in *Proceedings of the 31st International Electric Propulsion Conference, Ann Arbor, MI, 2009* (Electric Rocket Propulsion Society, Ann Arbor, MI, 2009), p. 199.
[16] B. Jorns, R. Sorenson, and E. Choueiri, Rev. Sci. Instrum. **82**, 123501 (2011).
[17] G. D. Severn, D. A. Edrich, and R. McWilliams, Rev. Sci. Instrum. **69**, 10 (1998).
[18] M. Sarfaty, S. D. Souza-Machado, and F. Skiff, Phys. Plasmas **3**, 4316 (1996).
[19] J. L. Kline, E. E. Scime, P. A. Keiter, M. M. Balkey, and R. F. Boivin, Phys. Plasmas **6**, 4767 (1999).
[20] J. Goree, M. Ono, and L. K. Wong, Phys. Fluids **28**, 2845 (1985).
[21] T. Stix, *Waves in Plasmas* (AIP, New York, 1992).